IJBPAS, January, 2024, 13(1): 34-48

ISSN: 2277–4998

International Journal of Biology, Pharmacy and Allied Sciences (IJBPAS)

'A Bridge Between Laboratory and Reader'

www.ijbpas.com

SYNTHESIS OF ZINC OXIDE AND ZINC/SILVER OXIDE NANOPARTICLES ASSISTED WITH N-HEXANE LEAF EXTRACT OF *STEPHANIA JAPONICA* LINN. AND ANTIBACTERIAL ACTIVITY AGAINST *S. AUREUS* AND *E. COLI*

KRISHNARAO KL[1*] AND RAJESWARI TR[2]

1: Research Scholar, Department of Chemistry, Acharya Nagarjuna University, Andhra Pradesh, India

2: Professor of Chemistry & Principal, Sri A.S.N.M. Government Degree College (A), Palakol, West Godavari (Dist), Andhra Pradesh, India

***Corresponding Author: Dr. Korampalli Lakshmi Krishnarao: E Mail: drklkrao123@gmail.com**

Received 19th Oct. 2022; Revised 16th Nov. 2022; Accepted 13th April 2023; Available online 1st Jan. 2024

https://doi.org/10.31032/IJBPAS/2024/13.1.7452

ABSTRACT

The development and practical application of nanotechnologies have increasingly attracted the attention of researchers due to the remarkable properties that can be achieved with materials when they are on the nanometric scale of size. The goal of this study was to create zinc oxide nanoparticles (ZnO NPs), ZnO nanoparticles with 0.25%(p/p) Silver added ($ZnO/Ag_{0.25}$ NPs), and ZnO nanoparticles with 0.5% (p/p) Silver added ($ZnO/Ag_{0.5}$NPs) using n-hexane extract of *Stephania japonica* Linn. leaf, which contained phenols, flavonoids. The synthesis of the ZnO and ZnO/Ag NPs was verified by XRD and TEM, and the NPs showed a hemispherical morphology and a particle size of less than 30 nm. The NPs were produced at temperatures between 300 and 600°C. This work also aims to study the antimicrobial activity of zinc oxide nanoparticles (ZnO NPs) and Zinc Oxide and Silver matrix nanoparticles ($ZnO/Ag_{0.25}$) against *Staphylococcus aureus* (*S. aureus*) and *Escherichia coli* (*E. coli*) bacteria. To evaluate the antimicrobial activity of ZnO NPs and $ZnO/Ag_{0.25}$, diffusion tests in solid media and Minimum Inhibitory Concentration (MIC) were performed. For ZnO NPs, the mean diameter of the inhibition halo was 1.1 ± 0.06 cm and 0.7 ± 0.15 cm for *S. aureus* and *E. coli*, respectively. The MIC of ZnO NPs determined in the present study to inhibit *S. aureus* ranges from 313.36µg

/ml and 626.64µg, while for *E. coli* it was not possible to determine the MIC because the solution saturated ZnO NPs is not sufficient to effectively inhibit this bacterium. When Silver was added to ZnO NPs, it decreased their bactericidal effect against *S. aureus*. The findings demonstrated that the ZnO NPs produced at 300°C (average size 9.9 nm) were more effective for the *in vitro* control of *S. aureus*. As for $ZnO/Ag_{0.25}$, there was no formation of inhibition halo, and it was not possible to determine the MIC for any of the bacterial strains under study, reaffirming the inability of bacterial inhibition of $ZnO/Ag_{0.25}$, without a supplying source of UV and/or visible light.

Keywords: *Stephania Japonica* Linn. leaf extract, zinc oxide, Silver, Antibacterial Activity

1. INTRODUCTION

Plants contain biomolecules, which have a high capacity for metal reduction. According to Ghotekar, *et al* (2019) **[1]** plant extracts can act as reducing agents and stabilizers in synthesizing different types of NPs. Additionally, the NPs are left with an organic coating, which improves their stability and decreases their aggregation **[2]**. In addition to being an environmentally friendly, economical technique that allows large-scale production of NPs, it is versatile and allows obtaining nanomaterials (NMs) with high purity and homogeneity **[4]**. The synthesis of NPs through the use of plant extracts has great potential for the bio-reduction of metallic cations of Silver, gold, copper and zinc or metallic oxides of zinc, Silver, titanium, aluminum etc., mainly used as antimicrobial agents against various human microorganisms and phytopathogens **[3]**. In general, one of the methodologies for the green synthesis of ZnO NPs is carried out as follows: dry leaves of some plant material are used, which are ground to obtain a powder material, this is mixed with some solvent (water or ethanol) and heated to a certain temperature for a certain time. The material obtained is then filtered and dried. To obtain the NPs, a stock solution of some chemical compound, such as zinc nitrate, is mixed with a certain amount of the extract if it is desired to prepare ZnO NPs, and the mixture is heated to a temperature between 80-100 °C, from which a precursor material is obtained, which is calcined at temperatures greater than 300 °C to finally obtain the desired oxide, take it to the characterization and final application.

Stephania japonica (*S. japonica*) belongs to Menispermiaceae family contains secondary metabolites such as polyphenolic compounds, quinones; that have therapeutic uses due to their antibacterial, anti-inflammatory, antifungal, and antioxidant properties **(Figure 1)**, which give them a potential use for disease control **[5]**.

Figure 1: ***Stephania japonica*** **Leaves**

In the literature it is mentioned that ZnO NPs are excellent candidates for use as antibacterial agent in pharma sector, due to their small size (<100 nm), they can interact easily with biological molecules **[6]**. It has been evaluated as an antibacterial agent on various Gram-positive and Gram-negative species. The antibacterial activity of ZnO NPs **[7]** made with plant extracts of *Olea europea* (48.2 nm), *Matricaria chamomilla* L. (65.4 nm), and *S. lycopersicum* (61.6 nm) has been assessed against *Xanthomonas oryzae*; the effectiveness of the NPs of ZnO depended on the extract used for synthesis, with those made with *Olea europea* being the best **[9]**. It has been proven that ZnO NPs combined with Silver increase their antibacterial capacity against microorganisms such as *B. subtilis*, *S. aureus*, *E. coli*, *Staphylococcus aureus*, *Pseudomonas aeruginos*a and *Klebsiella pneumoniae* **[8]**, with better antibacterial capacity than pure ZnO NPs, it was also shown that the increase in Ag content and the decrease in in particle size contribute significantly to antimicrobial efficiency **[10]**. Scanning electron microscopy confirmed the bacteriostatic effect of ZnO-Ag, which manifested itself in the arrest of cell division with significant cell elongation compared to the control **[9-10]**. Based on the aforementioned information, the current work was created with the aim of evaluating the ZnO, ZnO/$Ag_{0.25}$ and ZnO/$Ag_{0.5}$ nanoparticles produced with *S. Japonica* leaf extracts in vitro antagonistic effect against *S. aureus* and to analyse the effect of the NPs with the best antibacterial effect.

2 MATERIALS AND METHODS

2.1 Materials: Leaves of *S. Japonica* were collected during the spring-summer period in Vijayawada rural agricultural fields, 5 km from the municipality of Vijayawada, Andhra Pradesh, India. The leaves were dried at 80 °C for 24 hours, later they were ground dry in a blender and the biomass powder was obtained, which was used as raw material to prepare the extract that was used in the synthesis of nanoparticles. The extract was prepared by modifying the methodology reported by Ansari, *et al*., (2020) **[11]**. Extracts were prepared in

proportions of 0.5, 1, 2 and 3 grams of dry weight (DW) of biomass per 10 mL of solvent. The dry biomass was weighed depending on the proportion and placed in n-hexane (AR quality) purchased from Merck India, the suspension was placed in an ultrasound bath for 20 min for the extraction of secondary metabolites. Cell debris was then removed with Whatman filter paper number 1, the resulting solution was centrifuged at 15,000 rpm for 5 min, and the supernatant was recovered. The supernatant was stored in previously labelled glass bottles and refrigerated at -80 °C until use.

2.2 Characterization of the extract: The estimation of the number of total phenols present in the extract of *S. Japonica* was carried out with the Folin-Ciocalteu reagent according to the methodology of Li *et al* (2007) **[12]**. Total flavonoids were determined by the aluminum chloride colorimetric method according to the methodology of Li *et al* (2007). The concentration of chlorophyll A, B and total was determined by the method reported by Banu, (2015) **[13]**. The lyophilized extract of *S. Japonica* and the synthesized NPs were analysed by Fourier transform infrared spectroscopy (FTIR) to detect the characteristic peaks and their functional groups. The samples were measured in the wavelength range of 400 to 4000 cm-1 with a resolution of 4 cm-1; using the Nicolet Is 10 FT-IR spectrophotometer (Thermo Scientific). X-ray diffraction patterns (XRD) of the NPs were obtained using a Bruker AXS Kappa Apex2 CCD Diffractometer with a CuKα radiation source, operated at 44 mA and 40 Kv, in a scanning range of 10 to 80° in scale 2θ, at a speed of 0.02°/s; The equipment used was a Model FEI-Technai T20 Twin 200 KV instrument operated at an acceleration voltage of 300 Kv. For this characterization, a small amount of the sample was mixed with ethanol, then a micro drop of the solution was placed on a copper grid. TEM images were selected to count the particle size and generate the histograms, for this the ImageJ software was used and it was graphed with the OringinPro 2016 software.

2.2.1. Diffusion technique in solid medium from orifice

Diffusion in solid medium from an orifice was performed following the recommendations of the Clinical and Laboratory Standards Institute **[14]** using *Staphylococcus aureus* (ATCC 25925) and *Escherichia coli* (ATCC 25923) bacteria. First, the bacterial suspensions were cultured in Brain Heart Infusion broth (BHI, Himedia brand) for 24 h at 37±1 ºC in a bacteriological oven (Quimis brand, model Q316m5). Then, the bacterial colonies were isolated and after 24 h they were adjusted in sterile saline solution (0.85%) (NaCl, Merck

brand) to a concentration of 10^8 CFU/mL (Colony Forming Units per mL) using A spectrophotometer (Bel photonics, model 1105) was used at a wavelength of 619 nm. Mueller Hinton culture medium (Merck brand) was poured into the petri dishes and allowed to solidify. The bacteria under study were seeded in petri dishes with the aid of a sterile swab, seeding in three directions ensuring their total deposition on the culture medium. In each plate, three equidistant holes were made, with a diameter of approximately 0.8 cm, being deposited in these ZnO NPs and ZnO/$Ag_{0.25}$. It was incubated at 37±1 °C for 24 h and, after this period, the microbial growth inhibition halo formed according to Equation 1 was measured.

$$Inhibition\ Halo = D_{ex} - D_{in} \quad (1)$$

Where: D_{ex}: external diameter formed by the action of the antimicrobial agent on microorganisms (cm) D_{in}: diameter occupied by the antimicrobial agent (cm). The assay was performed in triplicate, and the mean value of inhibition halos was considered as a result.

2.2.2 Broth microdilution technique for the determination of the Minimum Inhibitory Concentration (MIC)

The MIC was determined using the methodology described by the Clinical and Laboratory Standards Institute (CLSI, 2012b), with some modifications. Standard solutions were prepared at 3133.3 µg /mL concentrations for ZnO NPs and 9533.3 µg /mL for ZnO/$Ag_{0.25}$ in ultrapure water, with homogenization performed by ultrasound (Eco-sonics brand, model Q1 .8/40 A). Such concentrations were determined from preliminary tests so that the solution was saturated and the compounds under study did not precipitate in the microwells of the analysis plate. Analogously to the solid medium diffusion assay, the bacteria used were *Staphylococcus aureus* (ATCC 25925) and *Escherichia coli* (ATCC 25923). 10 mL volumetric flasks were used to perform the serial dilution starting from the standard solution. 7 dilutions were performed as shown in **Table 1**. The assay was performed in 96-well sterile microplates (INLAB brand) with a "U" bottom, distributed in 8 rows named A through H and 12 columns.

Table 1: Solutions with different concentrations of ZnO NPs and ZnO/$Ag_{0.25}$NPs for the determination of MIC

line	ZnO NPs Conc. (µg/mL)	ZnO/$Ag_{0.25}$NPs Conc. (µg/mL)
A	2506.64	7626.64
B	1253.36	3813.36
C	626.64	2306.64
D	313.36	953.36
E	156.64	476.64
F	78.32	238.32
G	39.12	119.12
H	19.6	59.6

100 µl of BHI broth was placed in each of the microwells; then, in columns 1, 2 and 3 (characterized as the analysis triplicate) and line A, 100 µL of the most concentrated ZnO NPs solution was added, decreasing it in the subsequent lines in descending order. After that, 5 µL of microbial suspension with 10^8 CFU mL were added. In column 6 (negative control), 100 µL of BHI, 100 µL of ultrapure water and 5 µL of bacterial suspension (10^8 CFU /mL) were inserted to attest that the ultrapure water, used as a solvent, was not inhibiting microbial growth. In column 9 (positive control), 100 µL of BHI and 5 µL of bacterial suspension (10^8 CFU /mL) were inserted, in order to attest that the broth used allows the growth of the tested microorganisms; in column 12, only 100 µL of BHI was left, in order to certify its sterility (blank). In columns 4, 5, 7, 8, 10 and 11 nothing has been added. The microplates were then incubated in a microbiological oven at a temperature of 37±1 ºC for 20 h. After this period, 20 µL of TTC (2,3,5-triphenyltetrazole chloride, Sigma-Aldrich) were added to each microwell, an agent that promotes staining, allowing the visualization of bacterial growth. The microplates were taken to the bacteriological oven for another 4 h, and then removed to visualize the staining. The same analysis procedure was performed for $ZnO/Ag_{0.25}$.

3.0 RESULTS AND DISCUSSION

Preparation of *S. Japonica* leaf extract: To obtain the greatest number of secondary metabolites from *S. Japonica* leaf extract, the extraction of these was evaluated with n-hexane. Different proportions of biomass extracts were prepared with 5, 10, 20 and 30 grams of biomass (powdered dry leaves) per 10 mL of the solvent. 5g having 63.64mg Gallic Acid/gPS) in such way 10g (71.77 mg Gallic Acid/gPS), 20g (73.67 mg Gallic Acid/gPS) and 30g (77.06 mg Gallic Acid/gPS) respectively

3.1 Synthesis of ZnO and ZnO/Ag nanoparticles: For the synthesis of the NPs, two variables were evaluated: biomass concentration (0.5, 0.75, 1 and 2 g PS/10 mL of water) and temperature of calcination (300, 400, 500 and 600°C). The samples obtained after the calcination process at 500 ºC.

3.2 X-ray diffraction (XRD)

Figure 2 shows the X-ray diffraction patterns (XRD) of the ZnO NPs obtained at 500°C, with the *S. Japonica* extract at different biomass proportions. The presence of characteristic peaks located at 31.84, 34.44, 36.26, 47.56, 56.6, 62.9, 66.52, 67.96, 69.12 and 72.76° is observed in all the samples attributed to reflections of planes (100), (002), (101), (102), (110), (103), (200), (121), (201), and (202) with a hexagonal structure corresponding to ZnO (JCPDS No. 36-1451). Additionally, it is observed that as the amount of biomass

increases, small peaks appear located at 28.38, 40.54 and 50.14°, which correspond to the reflections (110), (200) and (211) of a phase identified as calcium (Ca) with cubic structure (JCPDS No. 10-0348), the intensity of these peaks also increases with increasing biomass (Estell *et al*., 1996). Also from the patterns, it can be seen that the main peaks corresponding to ZnO widen depending on the amount of biomass used to obtain the NPs. This broadening of the peaks is related to the size of the crystallite. Using the Scherrer equation (Cullity, 1956) it is possible to calculate this size according to the following expression:

$$D = K\lambda/\beta Cos\theta$$

Where,

D = Crystallite size in nm K = Shape constant equal to 1

λ = Wavelength of X-ray radiation (1.54 angstroms) β = Mean width of main peak

θ = Bragg angle

Figure 2 shows the X-ray diffraction patterns (XRD) of the ZnO NPs, $ZnO/Ag_{0.25}$ and ZnO/Ag0.5, obtained with two different calcination temperatures, 300 and 600 ºC (7a and 7b, respectively). The characteristic peaks of ZnO, already discussed above, are observed in the diffraction patterns. The average size of the crystallite obtained by XRD is 9.4 nm for the NPs obtained at 300 ºC and 22.7 nm for those obtained at 600 ºC. Additionally, in the diffraction patterns of the samples containing Silver, characteristic reflections located at 38.12, 44.3, 64.46 in planes (111), (200), (220) and (311) corresponding to a metallic Ag phase with crystalline structure are observed. FCC (JCPDS No. 04-0783).

In a study of ZnO/Ag nanocomposites, prepared using the precipitation method, diffraction peaks corresponding to two phases were presented. The main one was indexed as ZnO with hexagonal structure (JCPD No. 36-1451), while the other corresponded to metallic Ag with cubic structure centered on the face (JCPDS No. 04-0783), which evidences the formation of the ZnO/Ag nanocomposites. Therefore, Ag does not replace Zn^{2+} ions in its crystal structure, it is only as a phase independent of ZnO crystallites **[15]**. The results of XRD of the literature cited above, are similar to those obtained in this work, where there was no shift of the main peaks of ZnO and Ag in the samples obtained at different temperatures, showing that the green synthesis with extract of *S. Japonicais* possible to obtain ZnO/Ag nanocomposites to be studied and seek an opportunity for antibacterial activity study.

3.3 Transmission Electron Microscopy (TEM)

TEM micrographs and size histograms of the NPs synthesized by the *S. Japonica* extract with calcination treatments at 300 and 600 °C were obtained. **Figure 3** shows the TEM micrographs and histograms of the

ZnO, ZnO/$Ag_{0.25}$ and ZnO/$Ag_{0.5}$ NPs obtained at 300°C with hemispherical morphology. The ZnO NPs exhibited sizes between 5-30 nm, with an average of 12.73 ± 5 nm, of which more than 75% of these have a size less than 20 nm; while the ZnO/$Ag_{0.25}$ NPs presented a size distribution between 5-30 nm and an average of 12 ± 4.9 nm, where approximately 75% of these present a size smaller than 15 nm. For the ZnO/$Ag_{0.5}$ NPs, 75% of these had a size less than 20 nm with an average of 14.24 ± 6.9 nm. In recent studies, the optimization of the particle size in ZnO/Ag and ZnO/Cu samples has been reported **[21]**, it was found that there is a ZnO core with a uniform cover of Ag and Cu with particle sizes of 58.9 nm and 53.47 nm, respectively.

3.4 Ultraviolet Visible Spectrophotometry (UV-VIS)

Figure 4 shows the absorption spectrum of the synthesized ZnO;ZnO/$Ag_{0.25}$ nanoparticles. A broad absorption peak around 360-380 nm corresponds to a characteristic ZnO band **[17]**. Additionally, no other absorption peaks are observed in the spectrum, which confirms the purity of the nanoparticles obtained. The ZnO exhibits a maximum around 370 nm while using ZnO/$Ag_{0.25}$ has an absorption maximum at 373 nm. It is well known that a shift to longer wavelengths in the UV-VIS spectrum reflects an increase in particle size **[17]**. However, the two maximum wavelengths are close to each other, which is related to the average sizes between the obtained for both types of NPs obtained by XRD.

3.5 Light scattering in dynamic mode (DLS)

According to the histograms obtained for the two types of ZnO and ZnO/$Ag_{0.25}$ NPs synthesized; greater polydispersity can be seen when the nanoparticles were synthesized in the presence of Silver **(Figure 5)**. However, the average hydrodynamic size is between 1-5 nm in both cases. There are two main factors that contribute to the morphology and size of the final nanoparticles obtained under thermal conditions: the initial nucleation of the crystals and the solubility of the precursor in solvents with different vapor pressures **[18]**.

3.6 Antimicrobial studies

3.6.1. Diffusion technique in solid medium from orifice

Figure 6 shows the mean inhibition halo for ZnO NPs and ZnO/$Ag_{0.25}$NPs against *S. aureus* and *E. coli.*

Figures 6(a) and 6(b) show the mean inhibition halo formed by ZnO NPs against *S. aureus* and *E. coli* (c). These measurements were 1.1 0.06 cm and 0.7 0.15 cm, respectively. By measuring the size of the inhibitory halos produced by ZnO NPs, it is simple to confirm that they are more effective against *S. aureus* bacteria than *E. coli*. Unlike gram-negative bacteria

like *E. coli*, which have two outer layers, gram-positive bacteria like *S. aureus* only have one, making them more fragile. This is due to the ease with which exogenous chemicals can enter gram-positive bacterial cells and interact with the cytoplasmic membrane. These have a second membrane with a phospholipid bilayer structure that more effectively covers the inner cytoplasmic membrane, improving resistance to this type of bacterium.

Yamamoto, Osamu. (2001) **[19]** discovered that the mean particle diameter size is a major factor in the antimicrobial activity of zinc oxide nanoparticles against *E. coli*, with a halo of inhibition of 3.1± 0.01 cm for ZnO NPs with a particle size of 12 nm and a halo of inhibition of 2.7 ±0.01 cm for ZnO NPs with a particle size of 45 nm. Narayanan *et al*. (2012) discovered that the number of ZnO NPs is a positive factor when examined for antibacterial action. The authors utilised 20, 40, 60, 80, and 100 g of powder and achieved inhibition zones of 1.8, 1.9, 2.0, 2.0, and 2.1 cm for *S. aureus* and 1.3, 1.4, 1.6, 1.6, and 1.7 cm for *E. coli*, respectively. For ZnO/$Ag_{0.25}$-NPs, there was no inhibition halo for both bacteria under study. Some studies attest that ZnO/$Ag_{0.25}$-NPs have antimicrobial activity against gram-negative and gram-positive bacteria due to their photocatalytic activity, and this activity is associated with the electron/hole pairs generated in the photoexcitation process, which interact with the cell membrane of microorganisms, causing damage to it and causing leakage of minerals, proteins and genetic materials, culminating in cell death (Bonilla *et al*., 2013; Fu *et al*., 2005; Joo *et al*., 2005). However, such activity is limited to exposure of the compound to UV light and/or visible light, agents responsible for promoting the activation of the compound and consequent generation of electron/hole pairs. Therefore, without the presence of this agent, ZnO/$Ag_{0.25}$-NPs do not show effective antimicrobial activity, which is confirmed in the present study.

3.6.2. Minimum Inhibitory Concentration (MIC)

The study of MIC is important to determine the lowest concentration of solution capable of inhibiting the growth of microorganisms. **Figure 7** shows the results of the Minimum Inhibitory Concentration test for ZnO NPs when tested against *S. aureus* and *E. coli*, **Figure 7(a) and 7(b)**, respectively.

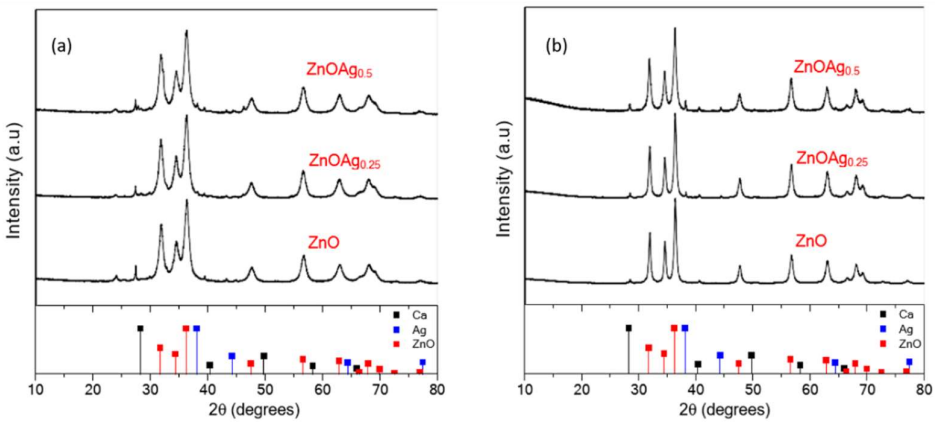

Figure 2: XRD patterns of ZnO, ZnO/Ag$_{0.25}$ and ZnO/Ag$_{0.5}$ nanoparticles using a biomass ratio of 0.75:10 p/v and calcination temperatures of 300°C (a) and 600 °C (b)

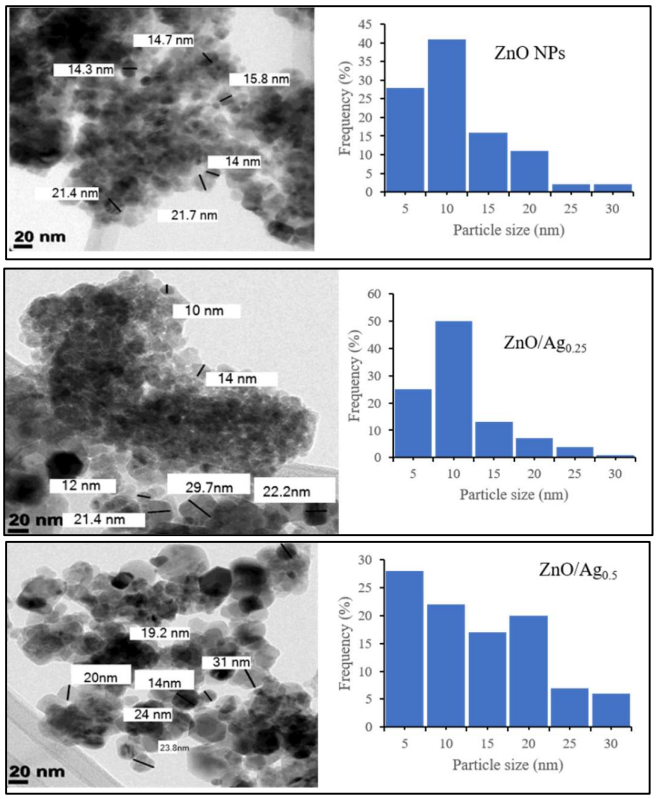

Figure 3: TEM micrograph and particle size distribution histogram of ZnO; ZnO/Ag$_{0.25}$ and ZnO/Ag$_{0.5}$ obtained at 600 °C using *S. Japonica* extracts

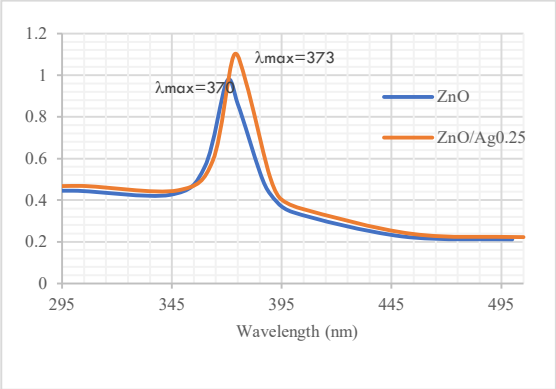

Figure 4: UV-VIS ultraviolet spectra of ZnO;ZnO/$Ag_{0.25}$ nanoparticles

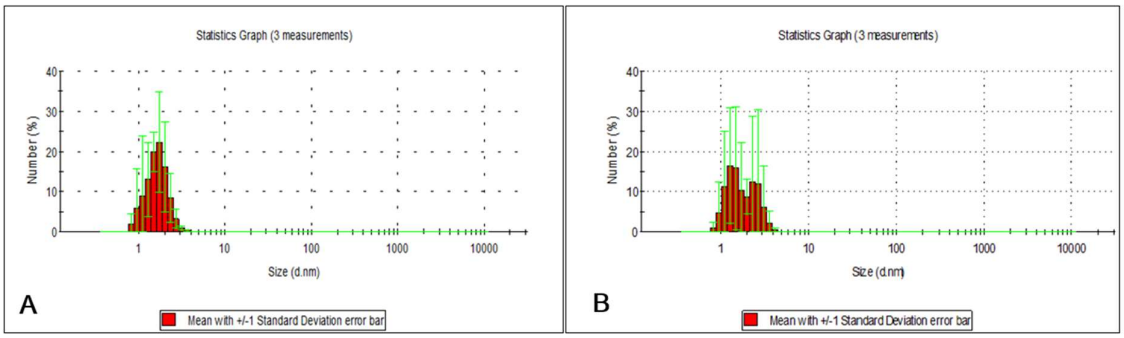

Figure 5: Average size distribution of A) ZnO NPs (B) ZnO/$Ag_{0.25}$ NPs

Figure 6: Results of the solid media diffusion test for (a) ZnO NPs/*S. aureus*; (b) ZnO/$Ag_{0.25}$/*S. aureus*; (c) ZnO NPs/*E. coli*; (d) ZnO/$Ag_{0.25}$/*E. coli*

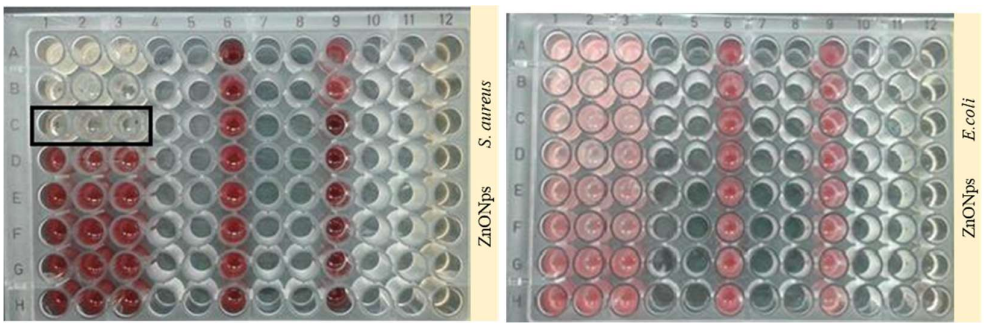

Figure 7: Results of the MIC test for ZnO NPs against (a) *S. aureus* and (b) *E. coli*

As can be seen in **Figure 7(a)**, the MIC of ZnO NPs to inhibit the growth of *S. aureus* at a concentration of 10^8 CFU /ml is between Line C and D, that is, between 313.36µg /ml and 626.64µg. For the bacterium *E. coli*, no inhibition of microbial cells was observed at any of the concentrations studied, that is, they were insufficient to inhibit the growth of said bacterium.

Although the diffusion assay in solid medium attested to the bactericidal and/or bacteriostatic capacity of ZnO NPs against *E. coli* through the diffusion mechanism, the MIC assay concentrations were insufficient to attest to the minimum inhibitory concentration for such bacteria. Due to the saturation of the ultrapure water/ZnO NPs solution at concentrations above that used, it cannot be increased, as the solution would precipitate at the bottom of the microwells, leading to a procedural error and, thus, compromising the analysis. Analogously to the one performed for ZnO NPs, the MIC test was carried out for $ZnO/Ag_{0.25}$, however, as already mentioned, $ZnO/Ag_{0.25}$, without an external light-supplying agent, does not present effective antimicrobial activity, as the photoexcitation does not happen and the inhibitory mechanism is compromised, a fact confirmed in the present analysis. It should be noted that, similarly to what happened with the ZnO NPs, it was not possible to use a more concentrated solution for the MIC tests, due to the saturation being reached and the deposition of the material at the bottom of the microwells, compromising the analysis. In a study carried out by Ghosh, *et al*. (2015), the authors focused light energy on ZnO/Ag and verified through the surface plating test that the concentration of ZnO/Ag that proved to be most effective to kill *E. coli* cells varying between 10^3 and 10^8 CFU /ml was 1 mg /ml. Furthermore, the study proved that $ZnO/Ag_{0.25}$ concentrations greater than 1 mg /ml reduce the killing efficiency for *E. coli* bacteria. This fact can be explained by the turbidity caused by the high concentration of $ZnO/Ag_{0.25}$ particles in suspension and the low penetration power of UV radiation, which reduces the intensity of radiation by the system.

4.0 CONCLUSION

The green synthesis of ZnO, $ZnO/Ag_{0.25}$ and $ZnO/Ag_{0.5}$ NPs with a particle size of less than 30 nm was possible, using as reducing agent the biocompounds of the n-hexane extract of *S. Japonica* leaves, making this methodology an economical, easy and environmentally friendly technique. The addition of Ag to the ZnO NPs improved their bactericidal effect; being the most effective for the in vitro control of *S. aureus*, the NPs of $ZnO/Ag_{0.25}$ with an average particle size of 9.9 nm, which allows us to accept the hypothesis. Additionally, these NPs improved seed germination and vigor at

the concentrations studied (250-1000 mg/L) without presenting possible phytotoxic effects. When the antimicrobial activity of ZnO NPs was evaluated by the solid medium diffusion assay, it was found that the average inhibition halo value was 1.06 ± 0.04 cm and 0.8 ± 0.16 cm for *S. aureus* and *E. coli*, respectively. The MIC of ZnO NPs determined in the study to inhibit *S. aureus* is between 313.36µg /ml and 626.64µg /ml. As for *E. coli*, it was not possible to determine the MIC. For ZnO/$Ag_{0.25}$-NPs, the manifestation of antimicrobial activity was not observed either by the solid medium diffusion test or by the MIC. The present study demonstrated that ZnO NPs have potential application to support materials whose antimicrobial functionality is desired to be inserted. Still, studies for photoexcited ZnO/$Ag_{0.25}$-NPs are suggested to verify if there is antimicrobial activity against the tested bacteria.

REFERENCES

[1] Ghotekar, Suresh & Pansambal, Shreyas & Pagar, Khanderao & Pagar, Trupti & Nikam, Amol. (2019). A Review on Plant Extract Mediated Green Synthesis of Zirconia Nanoparticles and Their Miscellaneous Applications. 1. 154-163. 10.33945/SAMI/JCR.2019.3.

[2] Kaushal, Priya & Verma, Naveen & Kaur, Kamaljit. (2021). Green Synthesis: An Eco-friendly Route for the Synthesis of Iron Oxide Nanoparticles. Frontiers in Nanotechnology. 3. 655062. 10.3389/fnano.2021.655062.

[3] Bao, Yunhui & He, Jian & Song, Ke & Guo, Jie & Zhou, Xianwu & Liu, Shima. (2021). Plant-Extract-Mediated Synthesis of Metal Nanoparticles. Journal of Chemistry. 2021. 1-14. 10.1155/2021/6562687.

[4] Castillo-Henríquez, Luis & Alfaro-Aguilar, Karla & Ugalde-Álvarez, Jeisson & Vega-Fernández, Laura & Montes de Oca-Vásquez, Gabriela & Vega-Baudrit, José. (2020). Green Synthesis of Gold and Silver Nanoparticles from Plant Extracts and Their Possible Applications as Antimicrobial Agents in the Agricultural Area. Nanomaterials. 10. 1763. 10.3390/nano10091763.

[5] Semwal, Deepak & Semwal, Ruchi & Semwal, Ravindra & Kothiyal, Sudhir & Singh, Gurjaspreet & Rawat, Usha. (2010). The genus Stephania (Menispermaceae): Chemical and pharmacological perspectives. Journal of Ethnopharmacology. 132. 369-383. 10.1016/j.jep.2010.08.047.

[6] Singh, Th & Sharma, Anirudh & Tejwan, Neeraj & Ghosh, Noyel & Das, Joydeep & Sil, Parames. (2021). A state of the art review on the synthesis, antibacterial, antioxidant, antidiabetic and tissue regeneration activities of zinc oxide nanoparticles. Advances in Colloid and Interface Science. 295. 102495. 10.1016/j.cis.2021.102495.

[7] 7-Abebe, Buzuayehu & Zereffa, E. & Tadesse, Aschalew & Murthy, H C

Ananda. (2020). A Review on Enhancing the Antibacterial Activity of ZnO: Mechanisms and Microscopic Investigation. Nanoscale Research Letters. 15. 190. 10.1186/s11671-020-03418-6.

[8] Mirhosseini, Mahboubeh & Firouzabadi, Fatemeh. (2013). Antibacterial activity of zinc oxide nanoparticle suspensions on food-borne pathogens. International Journal of Dairy Technology. 66. 10.1111/1471-0307.12015.

[9] Sirelkhatim, Amna & Mahmud, Shahrom & Seeni, Azman & Mohd Kaus, Noor Haida & Ann, Ling & mohd bakhori, Siti & Hasan, Habsah & Mohamad, Dasmawati. (2015). Review on Zinc Oxide Nanoparticles: Antibacterial Activity and Toxicity Mechanism. Nano-Micro Letters. 7. 10.1007/s40820-015-0040-x.

[10] Chauhan, Ankush & Verma, Ritesh & Kumari, Swati & Sharma, Anand & Shandilya, Pooja & Li, Xiangkai & Batoo, Khalid & Imran, Ahamad & Kulshrestha, S. & Kumar, Rajesh. (2020). Photocatalytic dye degradation and antimicrobial activities of Pure and Ag-doped ZnO using Cannabis sativa leaf extract. Scientific Reports. 10. 10.1038/s41598-020-64419-0.

[11] Ansari, Mohammad & Mahadevamurthy, Murali & Alzohairy, Mohammad & Almatroudi, Ahmad & Alomary, Mohammad. (2020). Cinnamomum verum Bark Extract Mediated Green Synthesis of ZnO Nanoparticles and Their Antibacterial Potentiality. Biomolecules. 10. 336. 10.3390/biom10020336.

[12] Li, Hua-Bin & Cheng, Ka-Wing & Wong, Chi-Chun & Fan, King-Wai & Chen, Feng & Jiang, Yue. (2007). Evaluation of antioxidant capacity and total phenolic content of different fractions of selected microalgae. Food Chemistry. 102. 771-776. 10.1016/j.foodchem.2006.06.022.

[13] Banu, Narasimhan. (2015). Extraction and estimation of chlorophyll from medicinal plants. International Journal of Science and Research (IJSR). 4. 209-212.

[14] Hsueh, Po-Ren & Ko, Wen-Chien & Wu, Jiunn-Jong & Lu, Jang-Jih & Wang, Fu-Der & Wu, Hsueh-Yi & Wu, Tsu-Lan & Teng, Lee-Jene. (2010). Consensus Statement on the Adherence to Clinical and Laboratory Standards Institute (CLSI) Antimicrobial Susceptibility Testing Guidelines (CLSI-2010 and CLSI-2010-update) for Enterobacteriaceae in Clinical Microbiology Laboratories in Taiwan. Journal of microbiology, immunology, and infection = Wei mian yu gan ran za zhi. 43. 452-5. 10.1016/S1684-1182(10)60070-9.

[15] Ebin, Burçak & Arıg, Elif & Ozkal, Burak & Gurmen, Sebahattin. (2012). Production and characterization of ZnO nanoparticles and porous particles by ultrasonic spray pyrolysis using a zinc nitrate precursor. International Journal of Minerals Metallurgy and Materials. 19. 651. 10.1007/s12613-012-0608-0.

[16] Skiba, Elżbieta & Michlewska, Sylwia & Pietrzak, Monika & Wolf, W.. (2020). Additive interactions of nanoparticulate ZnO with copper, manganese and iron in *Pisum sativum* L., a hydroponic study. Scientific Reports. 10. 13574. 10.1038/s41598-020-70303-8.

[17] Kasshun, Mideksa & Yadate, Alemayhu & Gemta, Abebe & Belay, Zerihun & Ramalingam, Murugan. (2020). Antimicrobial Activity of Chemical, Thermal and Green Route-Derived Zinc Oxide Nanoparticles: A Comparative Analysis. Nano Biomedicine and Engineering. 12. 10.5101/nbe.v12i1.p47-56.

[18] Wahab, Rizwan & Khan, Farheen & Gupta, Anoop & Wiggers, Hartmut & Saquib, Quaiser & Faisal, Mohammad & Ansari, Sabiha. (2019). Microwave plasma-assisted silicon nanoparticles: Cytotoxic, molecular, and numerical responses against cancer cells. RSC Advances. 9. 13336-13347. 10.1039/C8RA10185J.

[19] Yamamoto, Osamu. (2001). Influence of particle size on the antibacterial activity of zinc oxide. International Journal of Inorganic Materials - *Int J Inorg Mater*. 3. 643-646. 10.1016/S1466-6049(01)00197-0.

[20] Ghosh, Tanushree & Das, Anath & Jena, Bijaylaxmi & Pradhan, Chinmay. (2015). Antimicrobial effect of silver zinc oxide (Ag-ZnO) nanocomposite particles. Frontiers in Life Science. 8. 10.1080/21553769.2014.952048.

[21] Gurgur, Emmanuel & S., Oluyamo & Adetuyi, A. & Omotunde, Oluwatoyin & Okoronkwo, Afamefuna. (2020). Green synthesis of zinc oxide nanoparticles and zinc oxide–silver, zinc oxide–copper nanocomposites using *Bridelia ferruginea* as biotemplate. SN Applied Sciences. 2. 10.1007/s42452-020-2269-3.